Appl. Phys. B 81, 487–495 (2005)
DOI: 10.1007/s00340-005-1898-y

Applied Physics B
Lasers and Optics

M. PELTZ[1,✉]
J. BARTSCHKE[1]
A. BORSUTZKY[1]
R. WALLENSTEIN[1]
S. VERNAY[2]
T. SALVA[2]
D. RYTZ[2]

Harmonic generation in bismuth triborate (BiB_3O_6)

[1]Fachbereich Physik, Universität Kaiserslautern, Erwin-Schrödinger-Strasse 46, 67663 Kaiserslautern, Germany
[2]FEE GmbH, Struthstrasse 2, 55743 Idar-Oberstein, Germany

Received: 15 October 2004 / Revised version: 19 May 2005
Published online: 19 July 2005 •

ABSTRACT We report a study of second- and third-harmonic generation in BiB_3O_6 (BiBO). The effective nonlinearity, phase-matching angle, acceptance bandwidth, and walk-off are calculated and analyzed within the principal planes of the optical indicatrix. In the experiment, the phase-matched harmonic generation is investigated within the xz and yz planes. Also, the temperature dependence of the noncritical phase matching for laser radiation propagating along the z axis is measured for second-harmonic generation (SHG) at crystal temperatures of 25–265°C. The corresponding wavelengths of the laser radiation are in the range of 1.16 to 1.34 µm. In addition, SHG of 1342-nm radiation of a q-switched Nd:YVO_4 laser system is investigated for noncritical and critical phase matching. The achieved conversion efficiencies are 59% and 20%, respectively. Besides SHG, third-harmonic generation (THG) of 1064-nm, ns laser pulses is investigated. The measured conversion efficiency is as high as 34%. For THG the properties of BiBO are compared with those of BBO and LBO.

PACS 42.65.−k; 42.65.Ky; 42.70.Mp

1 Introduction

The generation of harmonics in nonlinear crystals is a well-established method to convert infrared laser light into visible or ultraviolet radiation. Although a variety of nonlinear optical materials are available today, there is still a strong interest in new nonlinear crystals with improved properties with respect to specific applications.

An example of such a new crystal is bismuth triborate, BiB_3O_6 (BiBO). BiBO is a monoclinic crystal of space group C2. Its existence was first mentioned by Levin and McDaniel in 1962 [1]. However, crystals of sufficient size and good optical quality were not grown until 1999 [2]. Important linear and nonlinear properties were reported by Hellwig et al. [3]. In 2001, Wesemann et al. presented an investigation of the crystal quality and the optical properties of BiBO for second-harmonic generation (SHG) of 1064 nm [4]. The crystal under investigation was cut at $\varphi = 90^\circ$ and $\Theta = -11^\circ$ in order to obtain a high effective nonlinearity. The crystal was of excellent optical homogeneity. Further advantageous properties for SHG of 1064 nm were low losses at the fundamental 1064 nm, a temperature acceptance of 2.17 K cm, an angular acceptance bandwidth of 1.22 mrad cm, and a high effective nonlinearity of 3.15 pm/V. These advantageous properties resulted in conversion efficiencies of 50% and 41% (limited by the available power) with nanosecond and picosecond Nd:YVO_4 laser pulses, respectively. In [5], Teng et al. reported an even higher efficiency of 67.7% for the SHG of picosecond pulses. Also, efficient intracavity SHG of 1.06 µm has been reported for ps pulses in a BiBO crystal with $\Theta = -11^\circ$ [6]. Recently, SHG of pulsed laser radiation in BiBO crystals was reported for different phase-matching directions [7]: it was observed that the conversion efficiencies are different for the phase-matching directions ($\varphi = 90^\circ$, $\Theta = 11^\circ$) and ($\varphi = 90^\circ$, $\Theta = -11^\circ$). A higher doubling efficiency was achieved for the phase-matching direction ($\varphi = 90^\circ$, $\Theta = -11^\circ$). In fact, the effective nonlinearity $d_{\text{eff}} = 2.2$ pm/V for $\Theta = 11^\circ$ has also been reported by Wesemann [8] as being smaller by about 30%.

Bismuth borate is of point group 2. Therefore, it is enantiomorphic and crystallizes in right- or left-handed forms. All crystals used in our experiments are right-handed crystals and all parameters given also correspond to this form.

In the first part of this paper, we report the calculation of the effective nonlinearity for type I and type II phase matching within the principal planes of the optical indicatrix of BiB_3O_6. The directions which provide the highest values are identified. In the second part, calculated results are presented for critical SHG in the principal planes. These results include the wavelength dependence of the direction for critical phase matching (CPM), the walk-off, and the angular and the spectral acceptance bandwidths. These calculations show that the most favorable directions for SHG in BiBO are within the xz and yz planes for $\Theta < 30^\circ$. Experimental results obtained for phase-matched frequency conversion in these two planes are compared with the theoretical predictions. Also, noncritical phase matching (NCPM) is demonstrated along the z axis for various temperatures. Efficient SHG of 1342-nm radiation of a Nd:YVO_4 laser is shown for critical and noncritical phase matching. Finally, efficient third-harmonic generation (THG) of 1064-nm radiation of a Nd:YVO_4 laser system is demonstrated and limitations are identified.

✉ Fax: +49-631-205-3906, E-mail: peltz@physik.uni-kl.de

2 Effective nonlinearity in bismuth borate

An important material parameter for efficient generation of harmonic radiation is the value of the coefficient d_{eff}. The knowledge of its value is therefore of primary interest.

The effective nonlinearity can be calculated by a projection of the d_{ijk} tensor on vectors of the electric field and the polarization according to

$$d_{\mathrm{eff}} = p_{\mathrm{i}}(\omega_3) d_{\mathrm{ijk}} e_{\mathrm{j}}(\omega_1) e_{\mathrm{k}}(\omega_2), \tag{1}$$

where $e_{\mathrm{i}}(\omega)$ is the ith component of the unit vector of the electric field of frequency ω_1 or ω_2. $p_{\mathrm{i}}(\omega_3)$ is the ith component of the unit vector of the generated polarization with frequency ω_3. In this calculation it is assumed that the d_{ijk} tensor is constant within the frequency range of interest.

In Ref. [3] the dijk tensor has been measured at a wavelength of 1079.5 nm. Also presented are the d_{eff} values as a function of the phase-matching angles (Θ, φ) for type I and type II SHG of 1079.5 nm. It is shown that due to the monoclinic symmetry there are two different d_{eff} values for the same phase-matching process in the yz plane. This is in accordance with experimental results presented in Refs. [4, 7, 8]. Effective nonlinearities for all phase-matching angles within the principal planes have not been published yet. For applications this is however of great interest because phase-matching angles within the principal planes can be calculated easily and the crystal fabrication is less difficult. In principle, the value of d_{eff} can be calculated using Eq. (1). In the special case of BiB_3O_6 the monoclinic symmetry introduces a rotation angle between the main axis e_{i} of the crystal physical coordinate system in which the dielectric tensor d_{ijk} is given and the axis system (x, y, z) of the main refractive indices $(n_{\mathrm{x}}, n_{\mathrm{y}}, n_{\mathrm{z}})$. (For a more detailed explanation of the coordinate systems, see Ref. [3].) To display the effective nonlinearity in the system of the refractive-index axis the components of the d tensor have to be transformed by a rotation of an angle ϕ around the x axis as in Ref. [3]. ϕ is a function of the wavelength and varies between the extreme values $\phi(365\,\mathrm{nm}) = 43.80^\circ$ and $\phi(1014\,\mathrm{nm}) = 47.18^\circ$. The effective nonlinearities calculated for type I and type II processes in the principal refractive-index planes are shown in Figs. 1 and 2, respectively. For the calculation it is assumed that the dielectric tensor d_{ijk} is constant with wavelength and for simplicity the value of the angle ϕ is constant. To illustrate the influence of the dispersion, the angle was calculated for the two extreme values of ϕ. Since we are exclusively discussing crystal properties within the principal planes, we are using the terminology of extraordinary (e) waves and ordinary (o) waves corresponding to the use in uniaxial crystals (see the similar usage of e and o in the discussion of phase-matching properties by Dmitriev [9]). This terminology has the advantage of including information about the polarization of the waves: e-waves are polarized within whereas o-waves are orthogonal to the actual phase-matching plane. For type I processes (Fig. 1) phase matched in the xz plane ($\varphi = 0^\circ$) the effective nonlinearity is considerably larger for processes with ee→o polarization, with a maximum value at the z axis ($\Theta = \varphi = 0^\circ$) of 2.72 pm/V (2.93 pm/V) for a coordinate-system rotation of $\phi = 43.8^\circ$ ($\phi = 47.18^\circ$). In this plane the d_{eff} values of

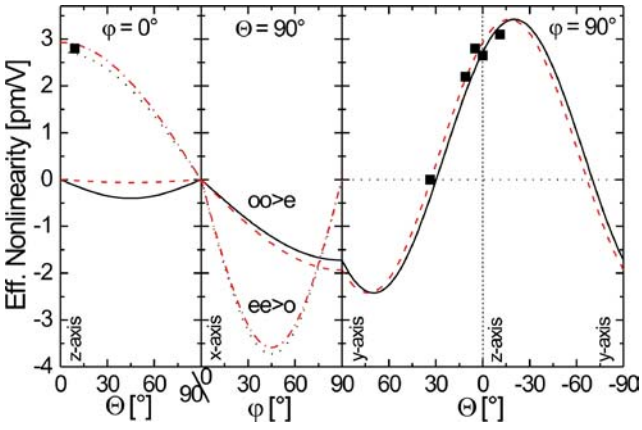

FIGURE 1 Calculated effective nonlinearity for type I ee→o and oo→e processes in BiBO for waves in the principal refractive-index planes. Note that the polarization changes from one plane to a neighboring plane. The calculations were performed for the two extreme dispersion angles $\phi = 43.8^\circ$ (*dash-dotted line* and *dashed line*) and $\phi = 47.18^\circ$ of the optical indicatrix

oo→e processes are in the range of -0.4 to -0.06 pm/V. In the xy plane ($\Theta = 90^\circ$) the d_{eff} values of ee→o and oo→e processes are remarkably high and amount to -3.89 pm/V (-3.73 pm/V) at $\varphi = 45^\circ$ and -1.73 pm/V (-1.93 pm/V) at $\varphi = 90^\circ$, respectively. In the yz plane an oo→e conversion is not feasible due to zero nonlinearity. Instead, a conversion with ee→o polarized waves provides nonlinearities varying between -2.42 pm/V and 3.42 pm/V. Due to a rotation of the coordinate system by an angle ϕ the extreme values of the nonlinearities are shifted from 0 and -90° to 70° (73°) and -20° (-17°), respectively. Therefore, there is no symmetry of the effective nonlinearity with respect to the z axis and there are two different values for $+\Theta$ and $-\Theta$.

Similar calculations have been done for parametric processes of type II (Fig. 2) considering eo→o (type IIa) and eo→e (type IIb) polarization schemes for dispersion angles of $\phi = 43.8^\circ$ and $\phi = 47.18^\circ$ of the optical indicatrix. In the xz plane the d_{eff} value for type IIa varies from 3.78 pm/V (3.61 pm/V) at $\Theta = 0^\circ$ to 0 pm/V at $\Theta = 90^\circ$. For type IIb the d_{eff} value shows a maximum at $\Theta = 45^\circ$ with $d_{\mathrm{eff}} = -2.60$ pm/V (-2.81 pm/V). In the xy plane the values

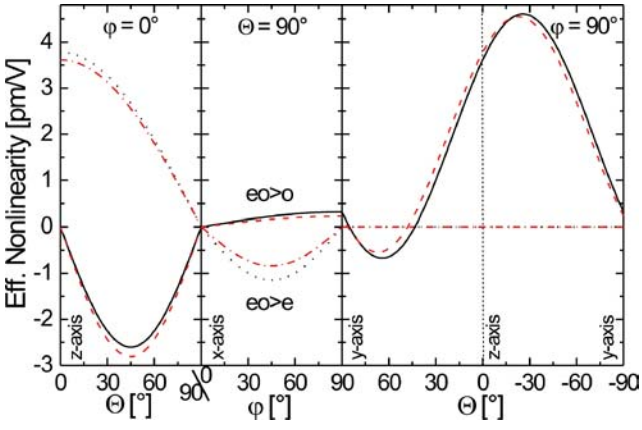

FIGURE 2 Calculated effective nonlinearity for type II eo→e and eo→o processes in BiBO for waves in the principal refractive-index planes. Note that the polarization changes from one plane to a neighboring plane. The calculations were performed for the two extreme dispersion angles $\phi = 43.8^\circ$ (*dash-dotted line* and *dashed line*) and $\phi = 47.18^\circ$ of the optical indicatrix

for both phase-matching (PM) schemes are rather small with d_{eff} (type IIa) ≤ -1.15 pm/V (-0.84 pm/V) and d_{eff} (type IIb) ≤ -0.32 pm/V (-0.23 pm/V). The nonlinearity for eo$\rightarrow$o PM in the yz plane is zero. The extreme nonlinearities for type IIb PM in the yz plane are located at $\Theta = 64^\circ$ (68°) and $\Theta = -27^\circ$ (-23°) with actual values of -0.67 pm/V (-0.54 pm/V) and -4.61 pm/V (-4.55 pm/V), respectively.

In summary, high values of the effective nonlinearity can be found for phase matching of types I and II in each refractive-index plane except for type IIa in the xy plane, where it is zero. Crystals in the yz plane should be cut at negative angles Θ to benefit from the higher nonlinearity.

3 Second-harmonic generation in BiBO

The knowledge of the effective nonlinearity for each direction as well as the possible phase-matching schemes for the specific type of interaction allows the determination of the range of angles for the most efficient frequency conversion. Phase matching is achieved when conservation of the energy ($h\omega_1 + h\omega_2 - h\omega_3 = 0$) and momentum ($\Delta\mathbf{k} = 0$) are met simultaneously. The wave-vector mismatch for a propagation direction Θ, φ of the interacting waves λ_1, λ_2, and λ_3 with the polarization e or o is given by

$$\Delta\mathbf{k} = \mathbf{k_1} + \mathbf{k_2} - \mathbf{k_3}, \tag{2}$$

with

$$\mathbf{k_j} = \frac{2\pi n_{\text{e,o}}(\lambda_j, \Theta, \varphi)}{\lambda_j}\mathbf{e}(\Theta, \varphi),$$

where n is the refractive index and e and o denote orthogonal polarizations. Sellmeier equations for the refractive indices have been published in Ref. [3].

Using these data the birefringent phase matching is calculated for collinear second-harmonic generation within the principal planes of the indicatrix. Figure 3 shows the fundamental wavelengths as a function of the crystal angle for the phase matching of type I and type II processes. Type I phase matching is possible for all wavelengths within the transparency range of the material. Most interesting are the angles Θ close to the z axis, where large tuning of the fundamental wavelength coincides with high values of the nonlinearity. Type II phase matching is limited at short wavelengths by 689 nm and at long wavelengths by the transparency limit. While the effective nonlinearity in the yz plane is zero, reasonable values of up to 2.5 pm/V are achieved in the xy and xz planes.

To verify the calculated wavelengths for type I phase-matching curves in the yz and xz planes, the wavelengths for phase-matched SHG are measured for different values of Θ. For this purpose a BiB_3O_6 crystal was cut orthogonal to the z axis. To have access to very large internal angles Θ from the z axis, the aperture of the crystal was 5.0×5.1 mm^2 and the crystal length was kept short ($L = 3.5$ mm). These dimensions allow angle tuning by more than $\pm 30^\circ$. Tunable fundamental wavelengths were generated using an optical parametric oscillator (OPO) system (GWU VisIR). This OPO system was pumped at 355 nm, the third harmonic of a 10-Hz repetition rate Nd:YAG laser. The OPO generated radiation at wavelengths from 410 nm to

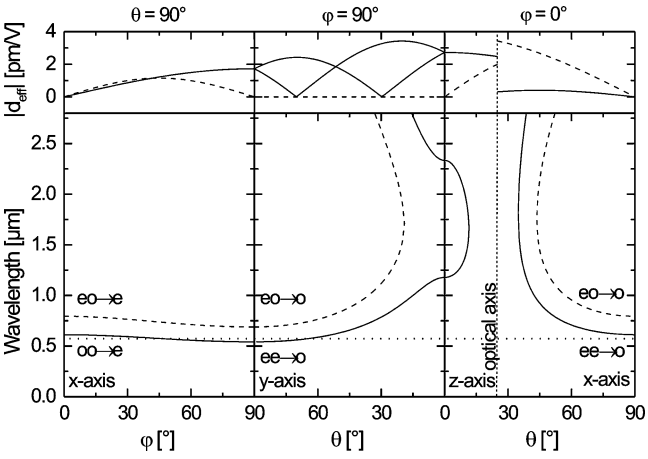

FIGURE 3 Calculated fundamental wavelengths as a function of the phase-matching angles for possible SHG for type I and type II processes in BiBO for waves in the principal planes. For easy comparison the corresponding effective nonlinearity is also given. (Phase matching and nonlinearity of type I: *solid line*; of type II: *dashed line*.) For wavelengths shorter than 572 nm (*horizontal dotted line*) the second-harmonic wave (< 286 nm) might already be absorbed significantly

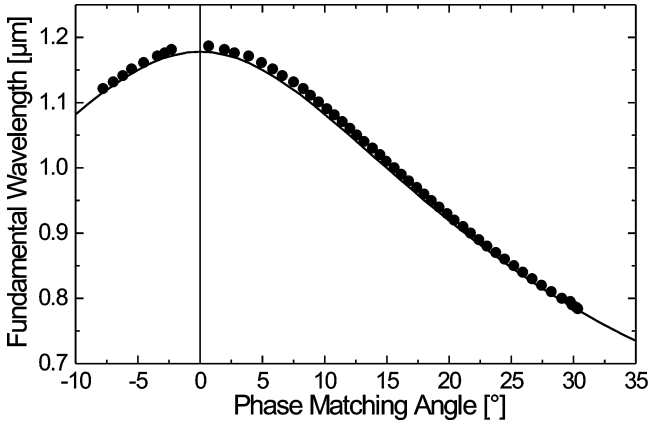

FIGURE 4 Second-harmonic generation with critical phase matching in the yz plane of BiBO. The *dots* represent the measured fundamental wavelength as a function of the polar angle Θ. The calculated phase-matching curve is represented by the *solid line*

2500 nm. The spectral width of the OPO wavelengths was about 4 cm^{-1} throughout the tuning range. The wavelength was measured with a LRL005 λ meter from Atos. The OPO radiation passed through a spatial filter and was focussed into the crystal to a spot size of 0.5 mm. The crystal was kept at room temperature, which was about 30°C. Figure 4 shows the measured wavelengths for angles Θ ranging from -10° to $+30^\circ$. By comparing the wavelengths for phase-matched SHG on both sides of the crystal, we found that the actual cut of the crystal was about -0.7° off the crystal's z axis. At normal incidence the measured fundamental wavelength for SHG was 1186 nm. The deviation of the measured and calculated wavelengths varies from 8 nm close to the z axis to about 2 nm at $\Theta = 30^\circ$. Regarding the xz plane (Fig. 5), the fundamental wavelengths for phase-matched SHG were measured for angles Θ from -8° to 11.3°. In this plane the measured phase-matching angle $\Theta = 0^\circ$ was identical with the angle of the crystal cut. The difference between the calculated and measured wavelengths ranges from 8 nm at normal incidence to about 10 nm at $\Theta = 10^\circ$.

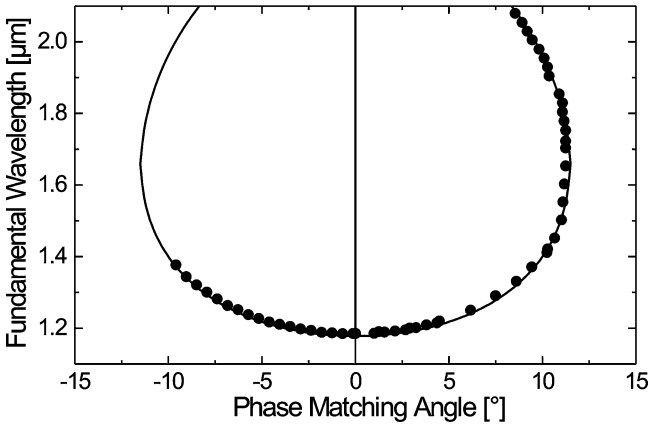

FIGURE 5 Second-harmonic generation with critical phase matching in the xz plane of BiBO. The *dots* represent the measured fundamental wavelength as a function of the polar angle Θ. The calculated phase-matching curve is represented by the *solid line*

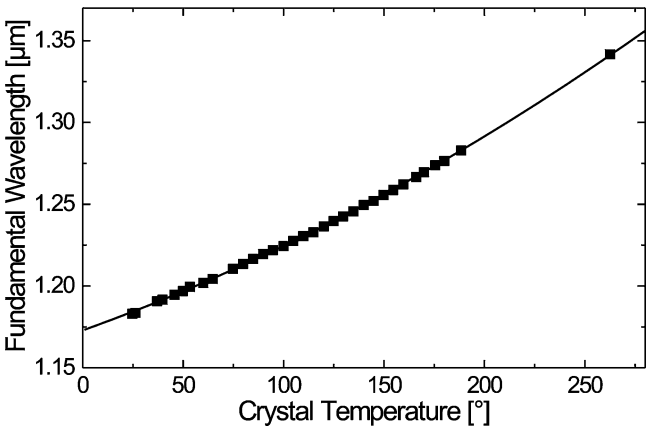

FIGURE 6 Second-harmonic generation with noncritical phase matching along the z axis in BiBO. The *squares* represent the measured fundamental wavelength as a function of the crystal temperature (*solid line*: polynomial fit)

Noncritical phase matching (NCPM) is of special interest because in this case beam interaction is free from beam walk-off. NCPM occurs along the main axes x, y, and z. As illustrated in Fig. 3 only type I PM is possible along the y and z directions due to the nonzero value of d_{eff}. Along the y axis the calculated phase matching is achieved by doubling 542 nm to 271 nm, a wavelength which is already partly absorbed. In the direction of the z axis phase matching should be possible at room temperature for 1178 nm and 2342 nm. The PM wavelength can be tuned by changing the refractive index via the crystal temperature. Since the temperature change of the refractive index has not been published yet, temperature tuning has to be determined experimentally. For this purpose the crystal was mounted in an oven with a maximum temperature near 200°C. In BiBO temperatures of up to 300°C are not critical. The fundamental wavelength was provided by the OPO system mentioned above. The crystal temperature was varied between 25°C and 190°C. In a second experiment with another oven we could reach a crystal temperature of up to 260°C. The results are shown in Fig. 6. The second harmonic was generated for wavelengths ranging from 1183.0 nm at 25°C to 1341.7 nm at 262.6°C. The solid curve was obtained by fitting a polynomial of second order to the measured data:

$$\lambda_{\text{SHG}}(T) = A + B(T - T_\circ) + C(T - T_\circ)^2, \tag{3}$$

with $A = 1.17286\,\mu\text{m}$, $B = 4.4011 \times 10^{-4}\,\mu\text{m/K}$, $C = 7.6454 \times 10^{-7}\,\mu\text{m/K}^2$, and $T_\circ = 273\,\text{K}$.

For real beams the phase mismatch Δk is nonzero due to the temperature fluctuations, the angular divergence of the beam, and the spectral width of the radiation. The finite acceptance width of the nonlinear crystal for these parameters can limit the conversion efficiency. The efficiency is reduced by a factor of two if the wave mismatch is $\Delta k = 0.886\pi/L$. The dependence of Δk on the parameter p in the second approximation is determined by the derivatives

$$\Delta k(p) = \Delta p(0) + \frac{\partial(\Delta k)}{\partial p}\Delta p + \frac{1}{2}\frac{\partial^2(\Delta k)}{\partial p^2}(\Delta p)^2, \tag{4}$$

with

$$p = \Theta, \varphi, \lambda, T,$$

with Δk derived from Eq. (2). Δp can be calculated by solving Eq. (4) and knowing the dependence of the refractive index n on the parameter p. The temperature acceptance has to be determined experimentally. Angular and spectral acceptances can be calculated using the Sellmeier equations in Ref. [3].

Figure 7 illustrates the angular and bandwidth acceptances for collinear phase-matched SHG within the three principal refractive-index planes. The typical spatial divergence of a focussed Gaussian laser beam is in the order of 1–10 mrad. In BiBO angular acceptances in the magnitude of Gaussian beams are found mainly close to the three axes, especially in the vicinity of the z axis. Fortunately, the width of the spectral acceptance is also largest around the z axis and coincides with the range of high nonlinearity.

Another parameter limiting the SHG efficiency is the spatial walk-off between the e-waves and the o-wave. The walk-off angle depends on the wavelength and is depicted in Fig. 8 for 400 nm and 2.5 µm. It can be seen that the walk-off in BiBO is relatively large in the yz and xz planes. The maximum values for the different planes at $\lambda = 400\,\text{nm}$ are $\rho(xy) = 1.2°$, $\rho(yz) = 4.6°$, and $\rho(xz) = 5.8°$.

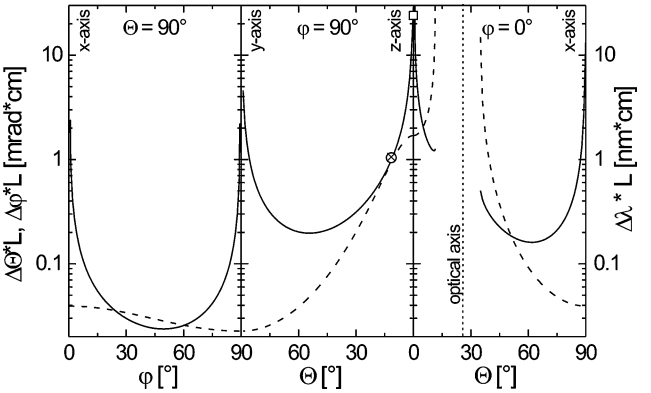

FIGURE 7 Calculated angular (*solid line*) and spectral (*dashed line*) acceptance widths for second-harmonic generation in the principal refractive-index planes of 10-mm-long BiBO crystals. *Open squares* are measured angular acceptance widths or given in Ref. [4]. *Crosses* correspond to the measured spectral acceptance of the same reference

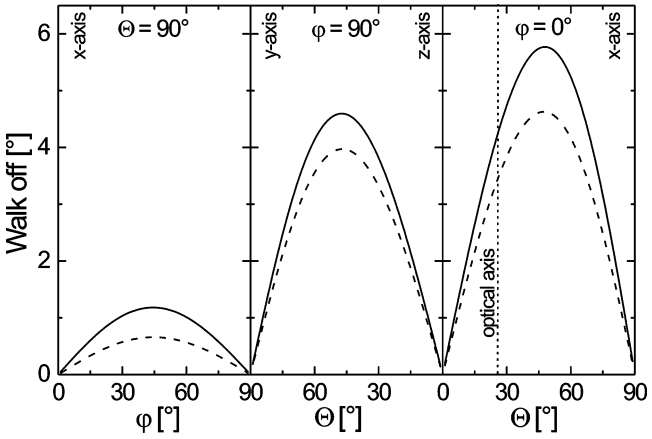

FIGURE 8 Walk-off angles calculated for 400-nm (*solid line*) and 2.5-μm (*dashed line*) radiation in the refractive-index planes

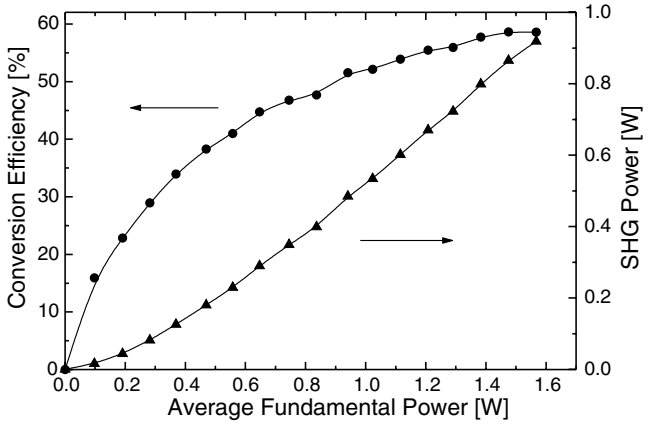

FIGURE 9 Generated second-harmonic power (*triangles*) of the 1342-nm radiation of a q-switched Nd:YVO_4 laser by NCPM in BiBO. The highest conversion efficiency (*dots*) of 59% is obtained at a fundamental pump power of 1.6 W

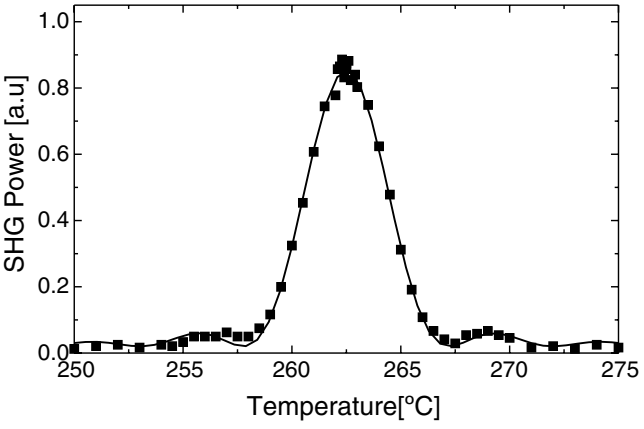

FIGURE 10 Power of the second harmonic generated at different crystal temperatures for propagation in the direction of the z axis. The temperature acceptance width of $\Delta T = 4.2$ K is obtained by a sinc^2 fit (*solid line*)

In conclusion, most promising collinear second-harmonic generation in BiBO can be achieved for type I critical phase matching within the yz and xz planes, where the values of the effective nonlinearity and the spectral and angular acceptances are relatively large. Since the walk-off is large in these planes a good spatial overlap of the interacting beams is restricted to phase matching along or in the vicinity of the z axis. For larger PM angles crystals of shorter length have to be used.

As an example of the capabilities of BiBO for SHG, frequency doubling of 1.342-μm radiation of a q-switched Nd:YVO_4 laser was investigated experimentally. Phase matching of the 1.3-μm line of Nd-doped laser crystals with BiBO can be achieved by NCPM along the z axis at temperatures near 250°C and by CPM in the xz plane at an angle Θ of approximately 9.1°.

A home-built diode-pumped acousto-optically q-switched Nd:YVO_4 laser provided pulses with a duration of 12 ns, a repetition rate of 10.1 kHz, and a maximum output power of 1.6 W. The laser pulses were focussed to a waist of $w_o = 77$ μm. For NCPM SHG a crystal with a length of $L = 10$ mm and an aperture (x, y) of $2.8 \times 3.0\,\mathrm{mm}^2$ was used. The crystal was mounted in an oven. Crystal and oven were positioned such that the focus was in the center of the crystal. To measure the power of the second harmonic it was separated from the fundamental by a Pellin–Broca prism. The values of the measured power are corrected for the Fresnel losses at the facets of the SHG crystal. At the highest fundamental power of 1.6 W, 920 mW of 671-nm radiation is produced (see Fig. 9). The conversion efficiency is 59%. Assuming a temporal Gaussian beam profile, the estimated effective nonlinearity is about 2.9 pm/V. This value is somewhat higher than the value calculated from the d tensor, which is about 2.8 pm/V (see Fig. 1). To determine the temperature acceptance for SHG of 1341.7-nm radiation the power of the generated second harmonic was measured for temperatures in the range from 250 to 275°C. As seen in Fig. 10, the phase matching with $\Delta k = 0$ occurs at 262.6°C. A sinc^2 fit to the data provides a temperature acceptance of $\Delta T L = 4.2$ K cm.

Correspondingly, we measured the generated second-harmonic power as a function of the angle of incidence. A sinc^2 fit to the measured data gave an angular acceptance of $\Delta\Theta L = 24$ mrad cm. This high value is in fair agreement with the calculated value of 30 mrad cm (Fig. 7). The spectral acceptance was not measured but the calculated value of $\Delta\lambda L = 1.7$ nm cm is large in comparison to the spectral width ($\Delta\lambda = 0.1$ nm) of the laser radiation.

Critical phase matching for the generation of 671 nm was performed by using a crystal cut in the xz plane at $\Theta = 9.1°$. The aperture was 3.0 mm × 4.2 mm. The length of the crystal was 5.1 mm; since the walk-off of the 671-nm radiation equals 1.5°, this limits the effective interaction length

$$L_e = \frac{\sqrt{\pi}\, w_0}{\tan\rho} \tag{5}$$

to about 6 mm. At 1.6 W of fundamental radiation the power of the generated SHG was 320 mW at 671 nm. This corresponds to a conversion efficiency of 20%. The lower conversion efficiency is mainly due to the shorter crystal length of 5.1 mm. The value of the estimated effective nonlinearity is 2.65 pm/V, which is in good agreement with the calculated effective nonlinearity of 2.8 pm/V. The angular and temperature acceptance bandwidths were measured as described above.

By fitting a sinc^2 function the values were determined to be $\Delta T L = 7.5\,\mathrm{K\,cm}$ and $\Delta\Theta L = 1.36\,\mathrm{mrad\,cm}$.

4 Third-harmonic generation in BiBO

Using Eq. (2), the relation between wavelength and phase-matching angle has been calculated for third-harmonic generation in BiBO within the principal planes of the optical indicatrix. Type I and type II phase matching (see Fig. 11) can be achieved for all wavelengths within the transparency range of the crystal. Type I PM is limited to $\Theta < 60^\circ$ in the yz plane and in the entire xz plane due to the transparency cut off for THG wavelengths shorter than 286 nm. Fortunately, the nonlinearity is highest in these planes. Type II PM can be separated into two parts by considering the polarization of the generating waves. For both type II PM schemes, PM is possible in all planes. In the yz plane, however, the value of d_{eff} is zero.

The angular acceptance for THG processes is shown in Fig. 12. The values were calculated for the three possible PM schemes in a BiBO crystal with a length of 10 mm. In all planes the acceptance is well above 1 mrad cm. The restrictions on the beam divergence can be met by most common (near-Gaussian) laser beams.

The spectral acceptance is illustrated in Fig. 13. The broadest spectral acceptance exists nears the z axis with values exceeding 10 nm cm. The lowest values are about 0.3 nm cm, for directions close to the x and y axes.

To confirm the properties of BiBO for third-harmonic generation, frequency tripling of 1064-nm laser radiation has been investigated experimentally. In these investigations two BiBO crystals have been used. Crystal no. 1 was cut at $\Theta = 33.7^\circ$ and crystal no. 2 at $\Theta = -33.7^\circ$. Both crystals provided type I phase matching in the yz plane. The size of these crystals was $2.9 \times 2.9 \times 5\,\mathrm{mm}^3$. The front facets were antireflection (AR) coated for the fundamental and the second harmonic (AR at 1064 nm and AR at 532 nm); the rear facets were antireflection coated for the generated third harmonic (AR at 355 nm).

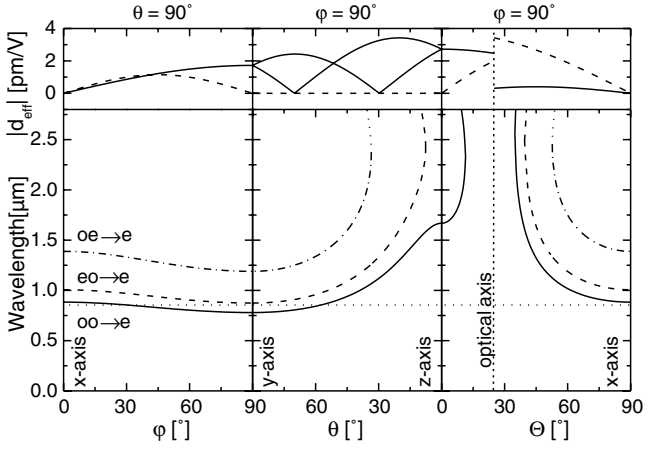

FIGURE 11 Calculated fundamental wavelengths as a function of the phase-matching angle for third-harmonic generation of types I and II in BiBO for waves in the principal refractive-index planes. The *dotted horizontal line* indicates the shortest wavelength which can be converted by THG to radiation within the transparency limit of the crystal

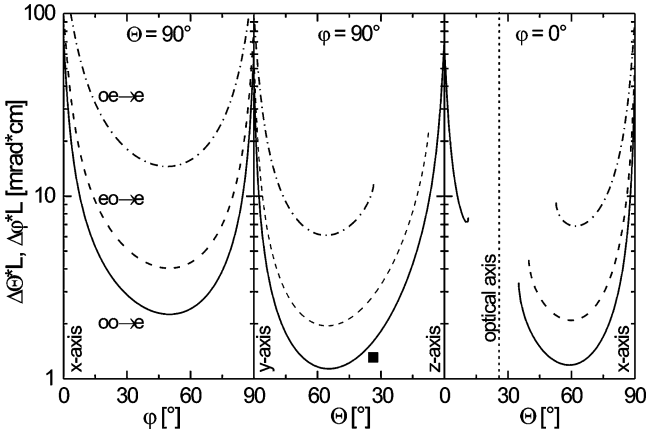

FIGURE 12 Angular acceptance width of type I and type II THG within the refractive-index planes in a 10-mm-long BiBO crystal (*solid line*, type I; *dashed* or *dash-dotted line*, type II)

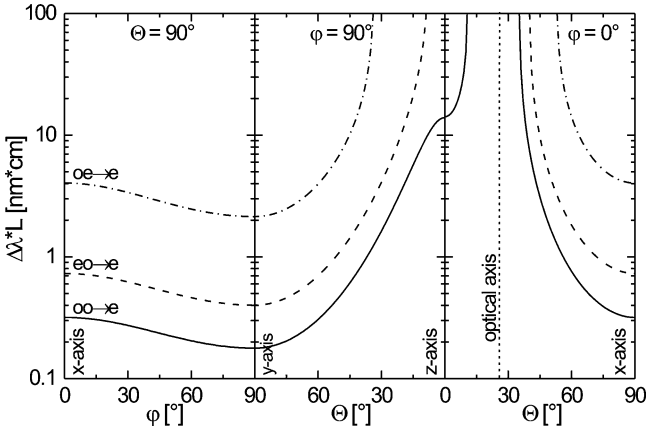

FIGURE 13 Spectral acceptance bandwidth for type I and type II THG within the refractive-index planes in a 10-mm-long BiBO crystal (*solid line*, type I; *dashed* or *dash-dotted line*, type II)

The experimental setup for the investigation of THG is shown in Fig. 14. The laser system is a q-switched Nd:YVO_4 laser system that generates 6-ns-long pulses at a repetition rate of 10 kHz. The diffraction-limited ($M^2 = 1.1$) laser radiation was frequency doubled (SHG) in a noncritically temperature phase matched LBO crystal. The fundamental and the second harmonic were separated by a dichroic beam splitter DS1 to allow for a rotation of the polarization of the second-harmonic wave by a half-wave plate. Two antireflection coated $f = 175$-mm lenses were used to focus the fundamental and the frequency-doubled beams to equal beam waists of $w_0 = 200\,\mu\mathrm{m}$. The beams were spatially superimposed by using the dichroic mirror DS2. The BiBO crystal was mounted on a rotation stage and was positioned at the beam waist. The

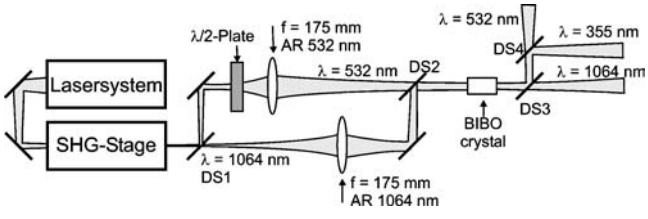

FIGURE 14 Experimental setup of the THG 355-nm generation

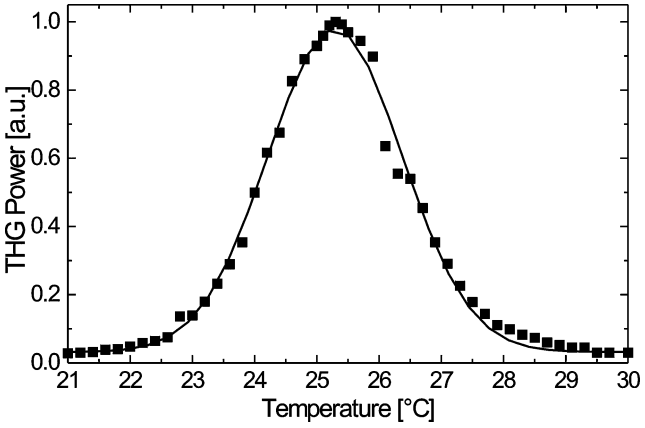

FIGURE 15 Generated TH (355 nm) power as a function of the temperature of a 5-mm-long BiBO crystal. The temperature acceptance width (FWHM) is $\Delta T = 2.2\,\mathrm{K}$ (*solid line*: sinc^2 fit)

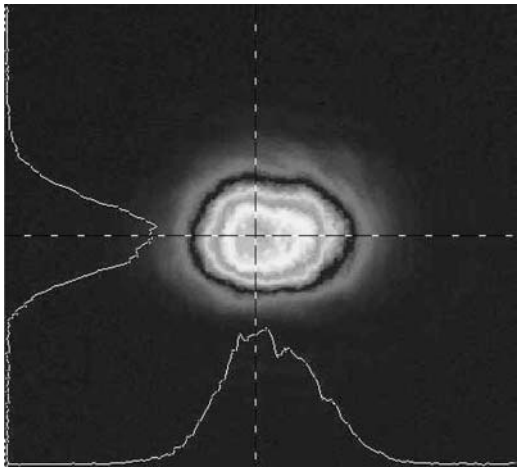

FIGURE 16 Intensity distribution and profiles of the generated 355-nm radiation at 1-W UV power

temperature of the crystal could be controlled with a Peltier with an accuracy of 0.1°C. The generated and transmitted radiation were separated by two dichroic mirrors (DS3 and DS4).

Phase-matched THG could be achieved with crystal no. 1 but with output powers around 10 mW for a total pump power of 1 W. This was expected since as seen from Fig. 1 the calculated effective nonlinearity is very small (0.2 pm/V). In comparison, the calculated value for d_{eff} for crystal no. 2 is 3.1 pm/V. This crystal was thus used exclusively in the following experiments.

In order to measure the temperature acceptance of the THG process the crystal was adjusted for highest output power at a crystal temperature of 25°C. The dependence of the third harmonic (TH) output power on the crystal temperature is shown in Fig. 15. This dependence shows a FWHM of 2.2 K. The temperature acceptance for THG of 1064-nm radiation is therefore 1.1 K cm.

In a similar way the angular acceptance was determined by measuring the output power in dependence on the phase-matching angle. According to a sinc^2 fit the external angular acceptance is $\Delta\Theta L = 1.84\,\mathrm{mrad}$. This corresponds to an angular acceptance width of $\Delta\Theta L = 0.52\,\mathrm{mrad\,cm}$.

The calculated walk-off for the e-polarized fundamental and the SH are 3.7° and 3.9°, respectively. Since the value of the walk-off is quite high the radius of the beam waist w_0 should not be below 200 µm. In this case the effective length L_{e} (Eq. (5)) is close to the length of 5 mm of the crystals used. As the crystal length is short compared to the confocal parameter of the focussed laser beams (which are 120 and 240 mm), the divergence of the beams inside the crystal is well below the angular acceptance.

For an average power of the fundamental laser beam of 4.5 W the generated SHG power was 2.55 W. The power of the remaining fundamental laser light was 1.95 W. With these input powers the average power of the generated 355-nm pulses was 1.75 W, which corresponds to an efficiency of 39%.

To investigate the beam quality of the generated third harmonic the spatial profile, the divergence, and the M^2 value of the UV beam were measured. The beam profile measured with a CCD camera is shown in Fig. 16. It has an almost Gaussian-like intensity distribution in the horizontal (yz plane of the crystal) and the vertical directions. Due to the walk-off the shape of the beam is slightly elliptical. The divergences in the horizontal and vertical directions were 1.6 mrad and 1.0 mrad, respectively. The larger value in the horizontal direction is a result of the walk-off. The beam-propagation factor M^2 was measured with a beam profiler (Beamscope, Merchantek) for three different UV powers (Table 1).

UV power [mW]	$M^2_{\perp}$	$M^2_{\parallel}$
300	1.0	1.3
600	1.1	1.4
1300	1.2	1.5

TABLE 1 Beam-propagation factor M^2 for the 355-nm radiation for different generated UV powers. M^2 values were determined perpendicular ($M^2_{\perp}$) and parallel ($M^2_{\parallel}$) to the walk-off (yz) plane

With increasing power the M^2 value increased to $M^2_{\perp} = 1.2$ orthogonal and $M^2_{\parallel} = 1.5$ parallel to the (yz) walk-off plane. These results indicate the good beam quality of the generated UV radiation.

As the generated radiation at 355 nm is close to the transparency limit of BiBO the threshold for damaging the crystal is of high interest. In the experiments the energy and power densities were up to $0.36\,\mathrm{J/cm^2}$ ($62\,\mathrm{MW/cm^2}$) for the two pump waves and $0.14\,\mathrm{J/cm^2}$ ($18\,\mathrm{MW/cm^2}$) for the UV beam. At these energy and power densities no damage of the crystal has been observed. To find the damage threshold, we investigated the absorption of 355 nm in BiBO using the z-scan method. Moderate UV powers (in the range of 1 to 120 mW) were focussed into an uncoated BiBO sample (dimensions: $3 \times 3 \times 5\,\mathrm{mm^3}$; cut at $\theta = 33.7°$, $\varphi = 90°$). In the focus the beam waist was 30 µm × 30 µm. The crystal was moved in steps of 25 µm from −25 mm to 25 mm with respect to the focus position. For each crystal position the transmitted power was recorded. These measurements were performed separately for the two directions of the polarizations of the 355-nm beam. The data were corrected for Fresnel losses. Incident powers and transmitted powers were divided by the measured beam area at the corresponding crystal position. Figure 17 shows the measured values for a polarization within the yz plane (e-polarization, triangles) and a polarization

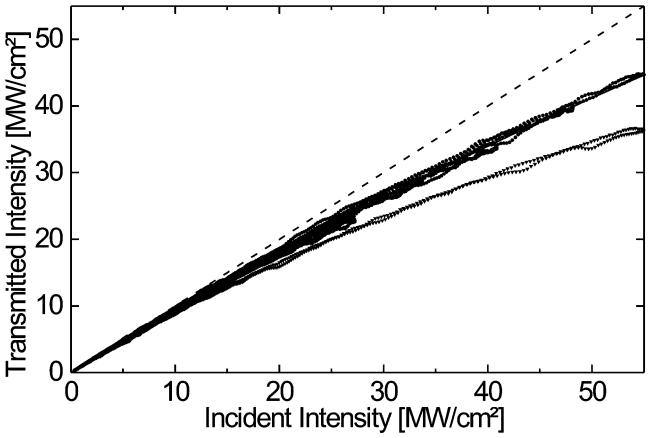

FIGURE 17 Transmitted 355-nm intensity as a function of the power intensity inside the BiBO crystal for e- and o-polarized radiation. The data were obtain by several z-scan measurements at different incident powers for the same focussing. The coefficients for linear and nonlinear absorption of 355-nm e-polarized (within yz plane) radiation are $\alpha = 0.095\,\mathrm{cm}^{-1}$ and $\beta = 1.60 \times 10^{-10}\,\mathrm{m/W}$ and $\alpha = 0.066\,\mathrm{cm}^{-1}$ and $\beta = 0.71 \times 10^{-10}\,\mathrm{m/W}$ for o-polarized (parallel to x axis) pulses

perpendicular to the yz plane (o-polarization, dots). The diagonal (dashed line) refers to zero absorption. By assuming the presence of linear absorption α and nonlinear absorption β, the change of the intensity $\mathrm{d}I$ over a length $\mathrm{d}z$ is given by

$$\mathrm{d}I = -(\alpha + \beta I)I\,\mathrm{d}z. \tag{6}$$

The equation is solved by

$$I(z) = \frac{\alpha}{\alpha + \beta I_0(1 - \mathrm{e}^{-\alpha z})} I_0\,\mathrm{e}^{-\alpha z}, \tag{7}$$

where I_0 is the incident intensity. A fit of the function (7) to the measured data provides values for the linear and nonlinear absorption of 355 nm in BiBO. For e-polarized waves $\alpha = 0.095\,\mathrm{cm}^{-1}$ and $\beta = 1.60 \times 10^{-10}\,\mathrm{m/W}$. For o-polarization $\alpha = 0.066\,\mathrm{cm}^{-1}$ and $\beta = 0.71 \times 10^{-10}\,\mathrm{m/W}$. Crystal damage was observed at power densities of $59\,\mathrm{MW/cm}^2$ and $55\,\mathrm{MW/cm}^2$ for e- and o-polarized waves, respectively. The UV radiation generated by THG is o-polarized. For this polarization the absorption is somewhat lower but still causes a relatively low damage threshold. As a consequence, the power densities have to be below the damage threshold by using weak focussing.

To compare the performance of BiBO with those of commonly used nonlinear optical materials, THG of 1064-nm radiation was investigated in BBO and LBO using the same experimental setup. The uncoated BBO crystals were 7- and 12-mm long and cut for type I and type II PM. In LBO PM was of type II. The crystal was 15-mm long with AR-coated facets. The experimental results and relevant material parameters are shown in Table 2. To allow a comparison of the results, the focus diameter of the incident laser radiation was kept at 400 µm × 400 µm. The TH output powers listed in Table 2 were achieved for a fundamental power of 4.5 W. The walk-offs in BiBO and both BBO PM configurations are very similar with 3.8°, 4.1°, and 4.5°. That of LBO is smaller by almost an order of magnitude with a value of 0.5°. The resulting effective crystal length is reduced to about 5 mm for BiBO and BBO. The effective length for LBO is $l_\mathrm{a} = 40$ mm, which exceeds the crystal length. The influence of the temperature and angular acceptances on the efficiency is negligible since temperature stabilization is easy to achieve and weak focussing (200 µm) reduces the divergence inside the crystal sufficiently. Besides the effective crystal length (which favors LBO), the value of the effective nonlinearity is most important for a high conversion efficiency. In this respect BiBO is clearly of advantage since the nonlinearity is 3.1 pm/V compared to 2.05 and 1.4 pm/V in BBO and 0.8 pm/V in LBO. The resulting efficiencies are 39% in BiBO, 36% in LBO, and about 22% in BBO. The corresponding UV powers are 1.75, 1.63, 0.94, and 0.85 W, respectively.

5 Summary and conclusion

In this paper the possibilities for phase-matched second- and third-harmonic generation in the new nonlinear material BiBO are analyzed. In addition, the values of the effective nonlinearities are calculated for directions within the three principal refractive-index planes. Values of up to 3.4 pm/V for type I and 4.6 pm/V for type II are obtained. Especially in the vicinity of the z axis, the nonlinearity is high. Due to the monoclinic symmetry the effective nonlinearity is different for negative or positive polar angles within the yz plane.

Calculations of the directions which provide phase-matched type I and type II harmonic generation show that SHG and THG are possible at all wavelengths within the

Nonlinear material	Crystal cut	Phase matching	Coating	Walk-off [°]	Geom. crystal length [mm]	Effective crystal length [mm]	Temp. acceptance [K cm]	Angular acceptance [mrad cm]	Effective nonlinearity [pm/V]	Max. TH power [W]	Efficiency [%]
BiBO	$\phi = 90°$ $\Theta = -33.7°$	Type I	AR	3.8	5	5.3	1.1	0.59	3.1	1.75	39
BBO	$\phi = 0°$ $\Theta = 31°$	Type I	–	4.1	7	4.9	16	0.26	2.05	0.94	23
BBO	$\phi = 30°$ $\Theta = 39°$	Type II	–	4.5	12	4.5	13	0.35	1.4	0.85	21
LBO	$\phi = 90°$ $\Theta = 42.7°$	Type II	AR	0.5	15	40		3.15	0.8	1.63	36

TABLE 2 Measurement results and important crystal parameters for third-harmonic generation with competing nonlinear materials. The TH power was measured at a fundamental pump power of 4.5 W focussed to a waist diameter of 400 µm

transparency range. The corresponding angular and spectral acceptances indicate that most favorable conditions exist in the yz and xz planes. The calculated walk-off in these planes is large with maximum values of up to 4.6° and 5.8°.

Experimentally, phase-matched SHG and THG are investigated for $0° < \Theta < 30°$ in the yz plane and $0° < \Theta < 11°$ in the xz plane at a crystal temperature of 30°C. The difference between the measured wavelength and the wavelength calculated by using the Sellmeier equations in Ref. [3] is up to 10 nm. This might be due to the large temperature tuning of the phase-matching wavelength of 0.44 nm/K. The temperature tuning was measured for noncritical PM along the y axis by varying the crystal temperature from 25 to 260°C. To demonstrate the advantage of BiBO for SHG, pulsed 1342-nm radiation was frequency doubled by noncritical and critical PM. The conversion efficiencies were 59% and 20%, respectively. The lower conversion efficiency obtained by critical phase matching is due to the shorter effective crystal length. The deduced effective nonlinearities are 2.65 pm/V and 2.8 pm/V. This is in good agreement with the calculated values. The temperature acceptances are 4.2 K cm and 7.5 K cm. The measured angular acceptances agree well with the calculated ones.

In a similar way, phase matching for third-harmonic generation was analyzed. First, the wavelength dependence of the phase-matching angle was calculated for type I and types IIa and IIb within the principal planes as well as the corresponding widths of the spectral and angular acceptances. The analysis indicated that phase matching is possible for all wavelengths within the transparency range of the crystal. Angular and spectral acceptances are quite large with values well above 1 mrad cm and 0.2 nm cm. Limitations are mainly due to zero nonlinearity for type II PM in the yz plane and the large walk-off.

Experimentally, THG of the 1064-nm fundamental of a $Nd:YVO_4$ laser system with 6-ns-long pulses and a repetition rate of 10 kHz was investigated. With a crystal cut in the yz plane at $\Theta = -33.7°$ a conversion efficiency of 39% was achieved. TH power at 355 nm of 1.75 W out of 4.5-W fundamental radiation was generated. The measured temperature acceptance was 1.1 K cm and the angular acceptance was 0.59 mrad cm. The generated UV radiation is nearly diffraction limited with a value of $M^2 = 1.2$ perpendicular and $M^2 = 1.5$ parallel to the walk-off plane. Also, the linear and nonlinear absorption coefficients have been determined for both polarizations. Due to the high nonlinear absorption the damage threshold is about 55 MW/cm^2. A comparison of BiBO with BBO and LBO for 355-nm generation showed that BiBO is a competitive material. Due to its high nonlinearity, strong focussing is not required, which reduces the influence of walk-off and intensity-dependent absorption.

In conclusion, BiBO is a suitable material for efficient second- and third-harmonic generation within a large wavelength range.

REFERENCES

1 E. Levin, C. McDaniel, J. Am. Ceram. Soc. **45**, 355 (1962)
2 P. Becker, J. Liebertz, L. Bohatý, J. Cryst. Growth **203**, 149 (1999)
3 H. Hellwig, J. Liebertz, L. Bohatý, J. Appl. Phys. **88**, 240 (2000)
4 V. Wesemann, M. Peltz, T. Bauer, J. L'Huillier, G. Bitz, R. Wallenstein, A. Borsutzky, T. Salva, S. Verny, D. Rytz, in *Conference on Lasers and Electro-Optics*, pp. 164–165 (Optical Society of America, Washington, DC, 2001)
5 B. Teng, J. Wang, Z. Wang, H. Jiang, X. Hu, R. Song, H. Liu, J. Wei, Z. Shao, J. Cryst. Growth **224**, 280 (2001)
6 C. Du, Z. Wang, J. Liu, B. Xu, B. Teng, K. Fu, J. Wang, Y. Liu, Z. Shao, Appl. Phys. B **73**, 215 (2001)
7 Z. Wang, B. Teng, K. Fu, X. Xu, R. Song, C. Du, H. Jiang, J. Wang, Y. Liu, Z. Shao, Opt. Commun. **202**, 217 (2002)
8 V. Wesemann, to be published
9 V. Dmitriev, G. Gurzadyan, D. Nikogosyan, *Handbook of Nonlinear Optical Crystals* (Springer, Berlin, 1999)